

# Ti–Sn, Zr–Sn, and Hf–Sn Heterodimetallic Complexes: Stabilizing Unsupported Group 4–Group 14 Metal–Metal Bonds

Matthias Lutz,<sup>†,‡</sup> Bernd Findeis,<sup>†</sup> Matti Haukka,<sup>‡</sup> Tapani A. Pakkanen,<sup>‡</sup> and Lutz H. Gade<sup>\*,†</sup>

*Laboratoire de Chimie Organométallique et de Catalyse (UMR 7513), Institut Le Bel, Université Louis Pasteur, 4 Rue Blaise Pascal, 67070 Strasbourg, France, and Department of Chemistry, University of Joensuu, 80101 Joensuu, Finland*

Received February 12, 2001

Reaction of the tripodal amido complexes  $[\text{MeSi}\{\text{SiMe}_2\text{N}(4\text{-CH}_3\text{C}_6\text{H}_4)\}_3\text{ZrCl}]$  and  $[\text{MeSi}\{\text{SiMe}_2\text{N}(4\text{-CH}_3\text{C}_6\text{H}_4)\}_3\text{HfCl}]$  with  $\text{LiSnPh}_3$  in toluene yielded the Zr–Sn and Hf–Sn complexes  $[\text{MeSi}\{\text{SiMe}_2\text{N}(4\text{-CH}_3\text{C}_6\text{H}_4)\}_3\text{ZrSnPh}_3]$  (**1**) and  $[\text{MeSi}\{\text{SiMe}_2\text{N}(4\text{-CH}_3\text{C}_6\text{H}_4)\}_3\text{HfSnPh}_3]$  (**2**), while attempts to synthesize the corresponding Ti–Sn complex resulted in the oxidative coupling of the stannate to give  $\text{Ph}_3\text{Sn–SnPh}_3$  and unidentified titanium species. More stable group 4–group 14 complexes were obtained by reaction of the triamido stannate complex  $[\text{MeSi}\{\text{SiMe}_2\text{N}(4\text{-CH}_3\text{C}_6\text{H}_4)\}_3\text{SnLi}(\text{OEt}_2)]$  with the metallocene dichlorides  $[\text{Cp}_2\text{MCl}_2]$  of all three titanium group metals, giving  $[\text{MeSi}\{\text{SiMe}_2\text{N}(4\text{-CH}_3\text{C}_6\text{H}_4)\}_3\text{SnM}(\eta^5\text{-C}_5\text{H}_5)_2(\text{Cl})]$  ( $\text{M} = \text{Ti}$ , **3**;  $\text{Zr}$ , **4**;  $\text{Hf}$ , **5**). X-ray diffraction studies of **4** and **5** established Zr–Sn and Hf–Sn bond lengths of 3.02313(17) and 2.9956(3) Å, respectively.

## Introduction

During the past three decades an enormous number of transition metal–group 14 heterodimetallic compounds have been synthesized.<sup>1–3</sup> Much of the interest in this area derives from the fact that the formation and transformation of transition metal-to-main group metal bonds are crucial steps in a variety of metal-mediated catalytic processes as well as in semiconductor growth.<sup>4,5</sup> On going from the late to the early transition metals, the polarity and, concomitantly, the reactivity of the metal–metal bonds increase significantly.<sup>3</sup> Whereas group 4–silicon compounds have found wide-ranging applications in some of these processes, their tin analogues remain extremely rare and thus poorly studied despite numerous efforts to develop their chemistry.<sup>1,6</sup> A principal problem appears to be that many of the synthetic strategies employed for M–Sn bond formation do not work well when M is titanium, zirconium, or hafnium.<sup>1–3</sup>

A fundamental difficulty in group 4–group 14 metal–metal bond formation is the existence of energetically low lying electron transfer reaction pathways from the group 14 metal to the early transition metal. This problem is not unlike the situation in early–late heterodinuclear transition metal complexes in which the metals from the two ends of the d-block are directly bonded to each other.<sup>7</sup> In this case, the choice of a set of chemically hard donor ligands on the early transition metal effectively suppresses the redox reactivity, and the integration of the donor functions into a polydentate ligand system additionally stabilizes such compounds.<sup>8</sup>

The tripodal amido ligands developed by us<sup>9–11</sup> were found not only to be ideally suited for that purpose but equally suitable as ligands for a group 14 metal complex fragment.<sup>12</sup> Triamidostannates were found to bind to potentially highly oxidizing metal centers such as  $\text{Ag}^{\text{I}}$ ,  $\text{Au}^{\text{II}}$ , and  $\text{Au}^{\text{III}}$  to give thermally stable heterometallic compounds.<sup>13</sup> The electronegative nitrogen substituents at divalent group 14 metal centers thus appear to

\* Corresponding author. E-mail: gade@chimie.u-strasbg.fr.

<sup>†</sup> Université Louis Pasteur.

<sup>‡</sup> University of Joensuu.

(1) Holt, M. S.; Wilson, W. L.; Nelson, J. H. *Chem. Rev.* **1989**, *89*, 11.

(2) Mackay, K. M.; Nicholson, B. K. In *Comprehensive Organometallic Chemistry*; Wilkinson, G. Stone, F. G. A.; Abel, E. W., Eds.; Pergamon Press: New York, 1982; Vol. 6, p 1043.

(3) Early examples of group 4–tin heterodimetallic complexes: (a) Croutts, R. S. P.; Wailes, P. C. *J. Chem. Soc., Chem. Commun.* **1968**, 260. (b) Kingston, B. F.; Lappert, M. F. *J. Chem. Soc., Dalton Trans.* **1972**, 69. (c) Creemers, H. M.; Verbeek, J. C.; Noltes, H. G. *J. Organomet. Chem.* **1968**, *15*, 125. The first structurally characterized Ti–Sn bond: Zheng, W.; Stephan, D. W. *Inorg. Chem.* **1988**, *27*, 2386.

(4) Cornils, B.; Herrmann, W. A., Eds. *Applied Homogeneous Catalysis with Organometallic Compounds*; VCH: Weinheim, 1996.

(5) Stringfellow, G. B.; Buchan, N. I.; Larsen, C. A. In *Materials Research Society Symposium Proceedings*; Hull, R., Gibson, J. M., Smith, D. A., Eds.; Materials Research Society: Pittsburgh, PA, 1987; Vol. 94, p 245.

(6) Woo, H. G.; Tilley, T. D. *Comments Inorg. Chem.* **1990**, *10*, 37.

(7) Reviews: (a) Stephan, D. W. *Coord. Chem. Rev.* **1989**, *95*, 41. (b) Wheatley, N.; Kalck, P. *Chem. Rev.* **1999**, *99*, 3379. (c) Gade, L. H. *Angew. Chem., Int. Ed.* **2000**, *39*, 2658.

(8) (a) Friedrich, S.; Memmler, H.; Gade, L. H.; Li, W.-S.; McPartlin, M. *Angew. Chem., Int. Ed. Engl.* **1994**, *33*, 676. (b) Findeis, B.; Schubart, M.; Platzek, C.; Gade, L. H.; Scowen, I. J.; McPartlin, M. *Chem. Commun.* **1996**, 219. (c) Jansen, G.; Schubart, M.; Findeis, B.; Gade, L. H.; Scowen, I. J.; McPartlin, M. *J. Am. Chem. Soc.* **1998**, *120*, 7239.

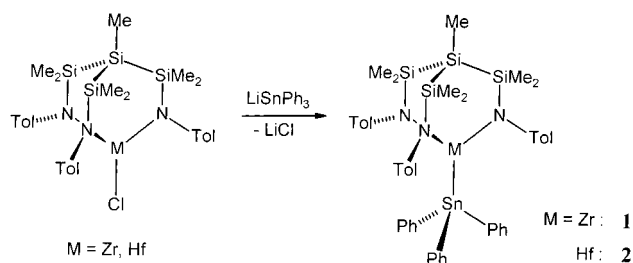
(9) Gade, L. H.; Mahr, N. *J. Chem. Soc., Dalton Trans.* **1993**, 489.

(10) (a) Gade, L. H.; Becker, C.; Lauher, J. W. *Inorg. Chem.* **1993**, *32*, 2308. (b) Memmler, H.; Gade, L. H.; Lauher, J. W. *Inorg. Chem.* **1994**, *33*, 3064.

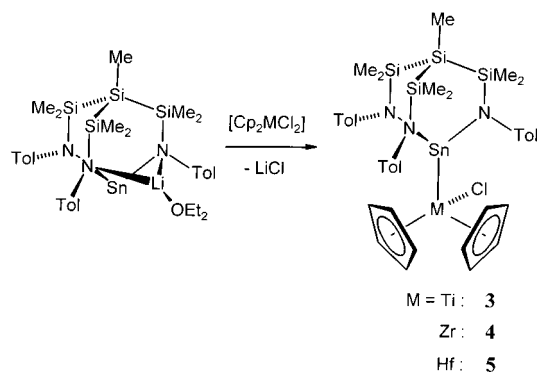
(11) Schubart, M.; Findeis, B.; Gade, L. H.; Li, W.-S.; McPartlin, M. *Chem. Ber.* **1995**, *128*, 329.

(12) (a) Hellmann, K. W.; Friedrich, S.; Gade, L. H.; Li, W.-S.; McPartlin, M. *Chem. Ber.* **1995**, *128*, 29. (b) Memmler, H.; Kauper, U.; Gade, L. H.; Stalke, D.; Lauher, J. W. *Organometallics* **1996**, *15*, 3637.

### Scheme 1. Syntheses of the Zr–Sn and Hf–Sn Complexes 1 and 2



### Scheme 2. Syntheses of the Group 4–Group 14 Complexes 3–5



stabilize the metals with respect to oxidation by a heterometal center to which they are bonded.

The aim of this study was to investigate whether the use of tripodal amido ligands in the complex fragments of either the group 4 or the group 14 metal would lead to stable heterodinuclear compounds whose isolation and complete structural characterization would be possible.

## Results and Discussion

Reaction of the previously reported tripodal amido complexes  $[\text{MeSi}\{\text{SiMe}_2\text{N}(4\text{-CH}_3\text{C}_6\text{H}_4)\}_3\text{ZrCl}]$  and  $[\text{MeSi}\{\text{SiMe}_2\text{N}(4\text{-CH}_3\text{C}_6\text{H}_4)\}_3\text{HfCl}]$ <sup>11</sup> with  $\text{LiSnPh}_3$  in toluene yielded, after workup, the yellow, microcrystalline Zr–Sn and Hf–Sn complexes  $[\text{MeSi}\{\text{SiMe}_2\text{N}(4\text{-CH}_3\text{C}_6\text{H}_4)\}_3\text{ZrSnPh}_3]$  (**1**) and  $[\text{MeSi}\{\text{SiMe}_2\text{N}(4\text{-CH}_3\text{C}_6\text{H}_4)\}_3\text{HfSnPh}_3]$  (**2**) (Scheme 1). Attempts to synthesize the corresponding Ti–Sn complex resulted in the oxidative coupling of the stannate to give  $\text{Ph}_3\text{Sn}–\text{SnPh}_3$  and unidentified titanium species, reflecting the generally greater tendency of titanium complexes to be reduced to Ti(III) intermediates than their heavier homologues.

The identity of compounds **1** and **2** was established by elemental analysis and their  $^1\text{H}$ ,  $^{13}\text{C}$ , and  $^{29}\text{Si}$  NMR spectra. The signal patterns in the latter indicate 3-fold molecular symmetry and support the structural proposals displayed in Scheme 1. As expected, both compounds are highly air and moisture sensitive and, if redissolved in polar solvents such as diethyl ether or THF, slowly decompose to give  $\text{Ph}_3\text{Sn}–\text{SnPh}_3$  as the only identifiable species.

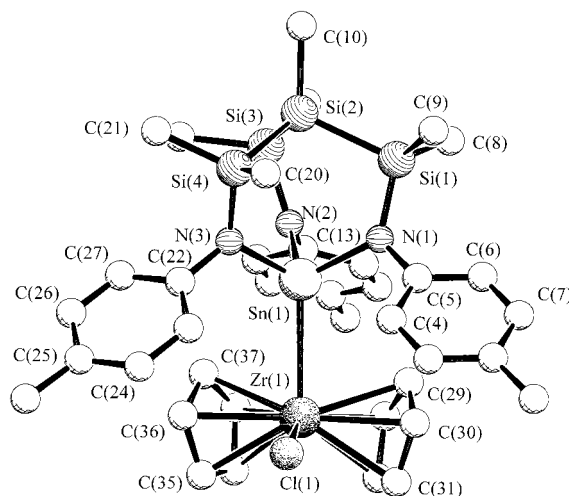


**Figure 1.** Molecular structure of compound **4**. The principal bond lengths and angles are listed in Table 1.

With the aim of obtaining heterodinuclear complexes of greater stability, the inverse coupling strategy was chosen. To this end, the previously characterized tri-amido stannate complex  $[\text{MeSi}\{\text{SiMe}_2\text{N}(4\text{-CH}_3\text{C}_6\text{H}_4)\}_3\text{SnLi}(\text{OEt}_2)]$ <sup>13</sup> was reacted with the metallocene dichlorides  $[\text{Cp}_2\text{MCl}_2]$  of all three titanium group metals. Nucleophilic substitution of one of the chloro ligands in the metallocene dichlorides occurred cleanly in all three cases, yielding the corresponding dinuclear complexes as thermally stable solids (Scheme 2).

Elemental analyses as well as the NMR spectroscopic data are consistent with their formulation as  $[\text{MeSi}\{\text{SiMe}_2\text{N}(4\text{-CH}_3\text{C}_6\text{H}_4)\}_3\text{SnM}(\eta^5\text{-C}_5\text{H}_5)_2(\text{Cl})]$  ( $\text{M} = \text{Ti}$ , **3**;  $\text{Zr}$ , **4**;  $\text{Hf}$ , **5**), and the molecular structures are shown in Scheme 2. As with compounds **1** and **2** we had difficulties in our attempts to record  $^{119}\text{Sn}$  NMR spectra of these complexes. We noticed this difficulty previously in compounds in which the transition metal–tin bond is very polar and in which the tin atom is coordinated to amido-N atoms.

To obtain insight into the detailed molecular structures of this type of complexes and to compare the analogous zirconium and hafnium species, single-crystal X-ray structure analyses of both **4** and **5** were carried out. Their molecular structures are depicted in Figures 1 and 2, and a comparative listing of their metric parameters is given in Table 1.

The structures are isomorphic and were solved as racemic twins in the orthorhombic space group  $P2_12_12_1$ . Since the molecular structures of **4** and **5** are virtually identical, they will be discussed together. The tripodal-amido-tin unit is characterized by its rigid cage structure as found in related tin complexes previously characterized by us. The peripheral tolyl groups adopt a “lamp shade” arrangement to make space for the  $\text{Cp}_2\text{MCl}$  fragment bonded through a metal–metal bond. The Zr–Sn bond length in **4** of 3.02313(17) Å is significantly longer than the sum of the covalent radii of the two metals as given by Pauling ( $\approx 2.85$  Å).<sup>14</sup> However, it is in the same range as the Zr–Sn distances in  $[\text{Zr}(\text{CO})_5(\text{SnMe}_3)_2]^{2-}$  [3.011(3) Å] and  $[\text{Zr}(\text{CO})_4(\text{dppe})-$

(13) (a) Findeis, B.; Gade, L. H.; Scowen, I. J.; McPartlin, M. *Inorg. Chem.* **1997**, *36*, 960. (b) Findeis, B.; Contel, M.; Gade, L. H.; Laguna, M.; Gimeno, M. C.; Scowen, I. J.; McPartlin, M. *Inorg. Chem.* **1997**, *36*, 2386.

(14) Pauling, L. *The Nature of the Chemical Bond*, 2nd ed.; Cornell University Press: Ithaca, NY, 1960.

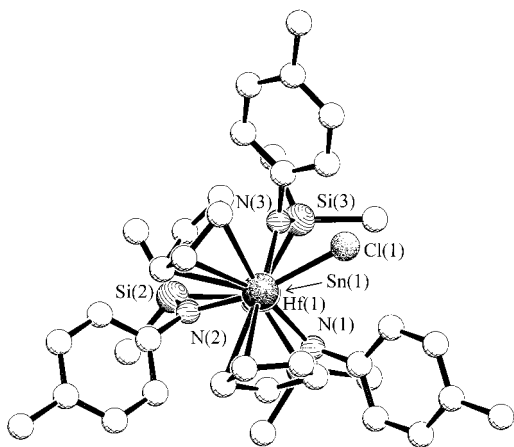


**Figure 2.** Molecular structure of compound **5**. The principal bond lengths and angles are listed in Table 1.

**Table 1. Principal Bond Lengths (Å) and Interbond Angles (deg) of Compounds **4** and **5****

<b>4</b>		<b>5</b>	
Sn(1)–N(1)	2.0973(14)	Sn(1)–N(1)	2.096(3)
Sn(1)–N(2)	2.0846(14)	Sn(1)–N(2)	2.081(3)
Sn(1)–N(3)	2.0913(14)	Sn(1)–N(3)	2.082(3)
Sn(1)–Zr(1)	3.02313(17)	Sn(1)–Hf(1)	2.9956(3)
Zr(1)–Cl(1)	2.4043(4)	Hf(1)–Cl(1)	2.3807(9)
Zr(1)–C(28)	2.4895(19)	Hf(1)–C(28)	2.464(5)
Zr(1)–C(29)	2.5206(19)	Hf(1)–C(29)	2.485(4)
Zr(1)–C(30)	2.5209(19)	Hf(1)–C(30)	2.505(4)
Zr(1)–C(31)	2.510(2)	Hf(1)–C(31)	2.481(5)
Zr(1)–C(32)	2.484(2)	Hf(1)–C(32)	2.465(5)
Zr(1)–C(33)	2.489(2)	Hf(1)–C(33)	2.479(5)
Zr(1)–C(34)	2.476(2)	Hf(1)–C(34)	2.466(5)
Zr(1)–C(35)	2.501(2)	Hf(1)–C(35)	2.495(5)
Zr(1)–C(36)	2.5216(19)	Hf(1)–C(36)	2.497(4)
Zr(1)–C(37)	2.522(2)	Hf(1)–C(37)	2.511(5)
N(2)–Sn(1)–N(3)	98.00(6)	N(2)–Sn(1)–N(3)	97.80(13)
N(1)–Sn(1)–N(2)	100.43(6)	N(1)–Sn(1)–N(2)	100.20(13)
N(1)–Sn(1)–N(3)	101.65(6)	N(1)–Sn(1)–N(3)	101.60(14)
N(2)–Sn(1)–Zr(1)	115.48(4)	N(2)–Sn(1)–Hf(1)	115.14(9)
N(3)–Sn(1)–Zr(1)	119.25(4)	N(3)–Sn(1)–Hf(1)	119.60(9)
N(1)–Sn(1)–Zr(1)	118.48(4)	N(1)–Sn(1)–Hf(1)	118.81(9)
Sn(1)–Zr(1)–Cl(1)	99.197(11)	Sn(1)–Hf(1)–Cl(1)	98.21(2)

SnMe<sub>3</sub>]<sup>–</sup> [3.061(2) Å] reported by Ellis and co-workers.<sup>15</sup> This observation is remarkable since the latter compounds are low oxidation state zirconium complexes with high coordination numbers and thus are expected to possess longer Zr–Sn bonds than those in **4**. It is quite likely that the length of the metal–metal bond in **4** is largely dictated by the repulsion of the ligand spheres of the two metal atoms. We note that metal–metal distances in the ZrSn<sub>2</sub> complex [Cp<sub>2</sub>Zr{Sn(CH(SiMe<sub>3</sub>)<sub>2</sub>)<sub>2</sub>}<sub>2</sub>] containing two stannylene units bonded to zirconium, which has been reported by Piers et al., are significantly shorter [2.8715(11) Å].<sup>16</sup> This is consistent with there being a partial double bond character of the metal–metal bonding in this compound.

Comparing the molecular structure of complex **5** with that of **4**, it is interesting to note that all bonds to hafnium in **5** are significantly shorter than those to the zirconium center in **4**. In particular, the Hf–Sn distance

of 2.9956(3) Å is contracted by almost 0.03 Å with respect to the analogous Zr–Sn bond and very similar to the Hf–Sn bond lengths determined in [(η<sup>6</sup>-C<sub>6</sub>H<sub>5</sub>-CH<sub>3</sub>)<sub>2</sub>Hf(SnMe<sub>3</sub>)<sub>2</sub>] reported by Green and co-workers.<sup>17</sup> There is one previous example in which two analogous Zr–Sn and Hf–Sn complexes were structurally characterized by X-ray diffraction, and this revealed a very similar relationship between the metal–metal bond lengths in both complexes. A decade ago, Ellis' group reported the syntheses and structures of [(Ph<sub>3</sub>Sn)<sub>4</sub>M(CO)<sub>4</sub>] (M = Zr, Hf) and found Zr–Sn and Hf–Sn distances of 3.086(1) and 3.063(1) Å, respectively.<sup>18</sup> The large intermetallic distances in these compounds are due to the low oxidation state of the group 4 metal and the high coordination number of 8.

A view along the metal–metal bond axis in **4** and **5** (Figure 2) illustrates the staggered arrangement of the ligands coordinated to the two distorted (pseudo)tetrahedrally coordinated metal centers. The fact that the intramolecular rotation around the M–Sn bond could not be frozen out in low-temperature NMR studies indicates that the barrier to such a rotation is lower than 10 kcal·mol<sup>–1</sup>. A closer inspection of the orientation of the tolyl groups with respect to the ligands coordinated at the Zr/Hf center in the crystal structures reveals that the two tolyl substituents bonded to N(1) and N(3) are slightly rotated toward each other, apparently to optimize π-arene·····H interactions with the two Cp rings at the group 4 metal.<sup>19</sup> No such interaction is possible for the third tolyl group at N(2), which lies between the two Cp rings of the early transition metal complex fragment.

Despite the long Zr–Sn and Hf–Sn bonds, both compounds **4** and **5** are remarkably stable. When they were heated at reflux in toluene, no appreciable decomposition was observed, and as solids they may be briefly handled in air, very likely due to the effective shielding of the highly polar metal–metal bond by the surrounding bulky ligand periphery.

## Conclusion

This study has shown that the strategy that was successfully employed for the stabilization of tin–transition metal bonds involving potentially oxidizing heterometal centers works equally well in the synthesis of novel group 4–group 14 metal complexes. Apart from the electronic properties of the amido ligand stabilizing the stannate units, the effective shielding of the metal–metal bond by the ligand framework and periphery of the tripod seems to play an important role. Current and future research in our laboratories is aimed at the activation of these systems toward polar and nonpolar organic substrates.

## Experimental Section

All manipulations and reactions were performed under argon (desiccant P<sub>4</sub>O<sub>10</sub>, Granusic, J.T. Baker) on a high-

(15) Ellis, J. E.; Yuen, P.; Jang, M. *J. Organomet. Chem.* **1996**, 507, 283.

(16) (a) Whittall, R. M.; Ferguson, G.; Gallagher, J. F.; Piers, W. E. *J. Am. Chem. Soc.* **1991**, 113, 9867. (b) Piers, W. E.; Whittall, R. M.; Ferguson, G.; Gallagher, J. F.; Froese, R. D. J.; Stronks, H. J.; Krygsman, P. H. *Organometallics* **1992**, 11, 4015.

(17) Cloke, F. G. N.; Cox, K. P.; Green, M. L. H.; Bashkin, J.; Prout, K. *J. Chem. Soc., Chem. Commun.* **1981**, 117.

(18) Ellis, J. E.; Chi, K.-M.; DiMaio, A.-J.; Frerichs, S. R.; Stenzel, J. R.; Rheingold, A. L.; Haggerty, B. S. *Angew. Chem., Int. Ed. Engl.* **1991**, 30, 194.

(19) Such an arrangement has been previously observed in early–late heterodinuclear complexes containing the tripod ligands: Gade, L. H.; Schubart, M.; Findeis, B.; Fabre, S.; Bezougli, I.; Lutz, M.; Scowen, I. J.; McPartlin, M. *Inorg. Chem.* **1999**, 38, 5282.

vacuum line using standard Schlenk techniques, or in a glovebox. All reaction flasks were heated prior to use using three evacuation–refill cycles. Solvents and solutions were transferred by cannula/septa techniques. Solvents were dried according to standard methods and saturated with argon.  $C_6D_6$  used for the NMR spectroscopic measurements was degassed by three successive “freeze–pump–thaw” cycles and stored over 4-Å molecular sieves. Solids were separated from suspensions either by centrifugation or by filtration through dried Celite. The centrifuge employed was a Rotina 48 (Hettich Zentrifugen, Tuttlingen, Germany), which was equipped with a specially designed Schlenk tube rotator.<sup>20</sup>

The  $^1H$ ,  $^{13}C$ , and  $^{29}Si$  NMR spectra were recorded on a Bruker AC 200 spectrometer equipped with a B-VT-2000 variable-temperature unit (at 200.13, 50.32, and 39.76 MHz, respectively).  $^1H$  and  $^{13}C$  data are listed relative to tetramethylsilane and were referenced using the residual protonated solvent peak ( $^1H$ ) or the carbon resonance ( $^{13}C$ ).  $^{29}Si$  data are relative to tetramethylsilane as an external standard. Infrared spectra were recorded on a Nicolet Magna IRTM 750 spectrometer.

Elemental analyses were carried out in the microanalytical laboratory of the chemistry department at the University of Würzburg using a Leco CHNS-932 microanalyzer. The compounds  $LiSnPh_3$ ,<sup>21</sup>  $[MeSi\{SiMe_2N(4-CH_3C_6H_4)\}_3ZrCl]$ ,<sup>11</sup>  $[MeSi\{SiMe_2N(4-CH_3C_6H_4)\}_3HfCl]$ ,<sup>11</sup> and the tris(amido)stannate  $[MeSi\{SiMe_2N(4-CH_3C_6H_4)\}_3SnLi(OEt_2)]$ <sup>13</sup> were prepared according to procedures reported in the literature. All other chemicals used as starting materials were obtained commercially and used without further purification.

**Preparation of  $[MeSi\{SiMe_2N(4-CH_3C_6H_4)\}_3ZrSnPh_3]$  (1).** A mixture of solid  $[MeSi\{SiMe_2N(4-CH_3C_6H_4)\}_3ZrCl]$  (761 mg, 1.15 mmol) and  $LiSnPh_3$  (421 mg, 1.18 mmol) was dissolved at room temperature in toluene (20 mL) and stirred for 2 h. Removal of the solvent in vacuo, extraction of the residue with pentane (25 mL), and centrifugation yielded a colorless solution, which was concentrated to about 5 mL and stored at  $-30^\circ C$ . Over a period of 2 days, compound **1** precipitated as a colorless microcrystalline solid. Yield: 714 mg (64%) of the analytically pure compound.  $^1H$  NMR (200.13 MHz,  $C_6D_6$ , 295 K):  $\delta$  0.14 (s, 3H,  $SiCH_3$ ), 0.36 (s, 18H,  $Si(CH_3)_2$ ), 2.33 (s, 9H,  $CH_3C_6H_4$ ), 7.01–7.18 (m, Ph, Tol), 7.61–7.68 (m, Ph).  $\{^1H\}^{13}C$  NMR (50.3 MHz,  $C_6D_6$ , 295 K):  $\delta$  -15.8 ( $SiCH_3$ ), 2.2 ( $Si(CH_3)_2$ ), 21.0 ( $CH_3C_6H_4$ ), 123.8 (Tol- $C^{2,6}$ ), 129.0 (Tol- $C^4$ ), 129.4 (Ph- $C^{3,5}$ ), 130.2 (Tol- $C^{3,5}$ ), 130.5 (Ph- $C^4$ ), 137.6 (Ph- $C^1$ ), 137.8 (Ph- $C^{2,6}$ ), 148.5 (Tol- $C^1$ ).  $\{^1H\}^{29}Si$  NMR (39.8 MHz,  $C_6D_6$ , 295 K):  $\delta$  -95.7 ( $SiCH_3$ ), -4.8 ( $Si(CH_3)_2$ ). Anal. Calcd for  $C_{46}H_{57}N_3Si_4SnZr$  [974.23]: C, 56.71; H, 5.90; N, 4.31. Found: C, 57.32; H, 6.11; N, 4.59.

**Preparation of  $[MeSi\{SiMe_2N(4-CH_3C_6H_4)\}_3HfSnPh_3]$  (2).** Reaction procedure as for **1** using 332 mg (0.44 mmol) of  $[MeSi\{SiMe_2N(4-CH_3C_6H_4)\}_3HfCl]$  and 159 mg (0.44 mmol) of  $LiSnPh_3$ . Compound **2** was obtained as a pale yellow microcrystalline solid in 48% (227 mg) yield.  $^1H$  NMR (200.13 MHz,  $C_6D_6$ , 295 K):  $\delta$  0.13 (s, 3H,  $SiCH_3$ ), 0.35 (s, 18H,  $Si(CH_3)_2$ ), 2.35 (s, 9H,  $CH_3C_6H_4$ ), 6.94–7.17 (m, Ph, Tol), 7.53–7.69 (m, Ph).  $\{^1H\}^{13}C$  NMR (50.3 MHz,  $C_6D_6$ , 295 K):  $\delta$  -16.1 ( $SiCH_3$ ), 2.3 ( $Si(CH_3)_2$ ), 20.9 ( $CH_3C_6H_4$ ), 124.4 (Tol- $C^{2,6}$ ), 129.0 (Tol- $C^4$ ), 129.2 (Ph- $C^{3,5}$ ), 130.1 (Tol- $C^{3,5}$ ), 130.4 (Ph- $C^4$ ), 137.6 (Ph- $C^1$ ), 137.8 (Ph- $C^{2,6}$ ), 148.4 (Tol- $C^1$ ).  $\{^1H\}^{29}Si$  NMR (39.8 MHz,  $C_6D_6$ , 295 K):  $\delta$  -99.1 ( $SiCH_3$ ), -5.3 ( $Si(CH_3)_2$ ). Anal. Calcd for  $C_{46}H_{57}HfN_3Si_4Sn$  [1061.50]: C, 52.05; H, 5.41; N, 3.96. Found: C, 52.47; H, 5.63; N, 4.09.

**Preparation of  $[MeSi\{SiMe_2N(4-CH_3C_6H_4)\}_3SnTi(\eta^5-C_5H_5)_2(Cl)]$  (3).** Toluene (15 mL) was added at  $-78^\circ C$  to a stirred mixture of  $[(\eta^5-C_5H_5)_2ZrCl_2]$  (215 mg = 0.86 mmol) and  $[MeSi\{SiMe_2N(4-CH_3C_6H_4)\}_3SnLi(OEt_2)]$  (632 mg = 0.86 mmol),

resulting in an immediate change of color from deep orange to dark red. The stirred reaction mixture was slowly warmed to room temperature over a period of 3 h. The  $LiCl$  formed in the reaction was separated by centrifugation, and the solvent volume of the centrifugate was reduced in vacuo to about 3 mL. Storing at  $-35^\circ C$  yielded a red solid, which was separated by decantation, washed with pentane (5 mL), and dried in vacuo to give 403 mg (54%) of **3**.  $^1H$  NMR (200.13 MHz,  $C_6D_6$ , 295 K):  $\delta$  0.27 (s, 3H,  $SiCH_3$ ), 0.60 (s, 18H,  $Si(CH_3)_2$ ), 2.19 (s, 9H,  $CH_3C_6H_4$ ), 5.32 (s, 10H,  $C_5H_5$ ), 6.98 (d, 6H,  $^3J_{HH} = 8.1$  Hz,  $H^{2,6}$  of  $CH_3C_6H_4$ ), 7.19 (d, 6H,  $^3J_{HH} = 8.1$  Hz,  $H^{3,5}$  of  $CH_3C_6H_4$ ).  $\{^1H\}^{13}C$  NMR (50.3 MHz,  $C_6D_6$ , 295 K):  $\delta$  -14.2 ( $SiCH_3$ ), 4.3 ( $Si(CH_3)_2$ ), 20.9 ( $CH_3C_6H_4$ ), 113.7 ( $C_5H_5$ ), 128.5 ( $C^{2,6}$ ), 129.6 ( $C^{3,5}$ ), 130.2 ( $C^4$ ), 150.5 ( $C^1$ ).  $\{^1H\}^{29}Si$  NMR (39.8 MHz,  $C_6D_6$ , 295 K):  $\delta$  -87.4 ( $SiCH_3$ ), 0.2 ( $Si(CH_3)_2$ ). Anal. Calcd for  $C_{38}H_{52}ClN_3Si_4SnTi$  [865.22]: C, 52.75; H, 6.06; N, 4.86. Found: C, 52.64; H, 6.42; N, 4.91.

**Preparation of  $[MeSi\{SiMe_2N(4-CH_3C_6H_4)\}_3SnZr(\eta^5-C_5H_5)_2(Cl)]$  (4).** Toluene (15 mL) was added at  $-78^\circ C$  to a stirred mixture of  $[(\eta^5-C_5H_5)_2ZrCl_2]$  (399 mg, 1.36 mmol) and  $[MeSi\{SiMe_2N(4-CH_3C_6H_4)\}_3SnLi(OEt_2)]$  (1.00 g, 1.36 mmol), resulting in an immediate change of color from pale yellow to orange. The stirred reaction mixture was slowly warmed to room temperature over a period of 3 h. The  $LiCl$  formed in the reaction was separated by centrifugation, and the solvent volume of the centrifugate was reduced in vacuo to about 3 mL. Storing at  $-35^\circ C$  yielded an orange solid, which was separated by decantation, washed with pentane (5 mL), and dried in vacuo to give 729 mg (59%) of **4**. Recrystallization from a saturated solution of **4** (125 mg, 0.14 mmol) in benzene (0.5 mL) afforded suitable single crystals for the structure determination. IR (KBr): 3105 vw, 3024 vw, 2958 w, 2892 vw, 1617 m, 1697 m, 1516 s, 1499 s, 1434 w, 1365 w, 1288 m, 1250 s, 1227 s, 1182 vw, 1112 w, 1020 m, 1017 m, 945 m, 915 s, 898 s, 814 ws, 778 s, 708 w, 685 w, 656 w, 633 vw  $cm^{-1}$ .  $^1H$  NMR (200.13 MHz,  $C_6D_6$ , 295 K):  $\delta$  0.30 (s, 3H,  $SiCH_3$ ), 0.64 (s, 18H,  $Si(CH_3)_2$ ), 2.18 (s, 9H,  $CH_3C_6H_4$ ), 5.37 (s, 10H,  $C_5H_5$ ), 7.02 (d,  $^3J_{HH} = 7.9$  Hz, 6H,  $H^{2,6}$  of  $CH_3C_6H_4$ ), 7.22 (d,  $^3J_{HH} = 8.1$  Hz, 6H,  $H^{3,5}$  of  $CH_3C_6H_4$ ).  $\{^1H\}^{13}C$  NMR (50.3 MHz,  $C_6D_6$ , 295 K):  $\delta$  -14.2 ( $SiCH_3$ ), 4.0 ( $Si(CH_3)_2$ ), 20.9 ( $CH_3C_6H_4$ ), 112.1 ( $C_5H_5$ ), 128.4 ( $C^{2,6}$ ), 129.9 ( $C^{3,5}$ ), 130.4 ( $C^4$ ), 151.2 ( $C^1$ ).  $\{^1H\}^{29}Si$  NMR (39.8 MHz,  $C_6D_6$ , 295 K):  $\delta$  -88.6 ( $SiCH_3$ ), -0.5 ( $Si(CH_3)_2$ ). Anal. Calcd for  $C_{38}H_{52}ClN_3Si_4SnZr$  [908.56]: C, 50.24; H, 5.77; N, 4.62. Found: C, 50.53; H, 5.92; N, 4.87.

**Preparation of  $[MeSi\{SiMe_2N(4-CH_3C_6H_4)\}_3SnHf(\eta^5-C_5H_5)_2(Cl)]$  (5).** An analogous procedure described to prepare **4**, using 432 mg (0.59 mmol) of  $[MeSi\{SiMe_2N(4-CH_3C_6H_4)\}_3SnLi(OEt_2)]$  and 224 mg (0.59 mmol) of  $[(\eta^5-C_5H_5)_2HfCl_2]$ , gave compound **5** as a bright yellow crystalline solid in 48% (276 mg) yield. IR (KBr): 3115 vw, 3024 vw, 2958 w, 2897 vw, 1610 m, 1516 m, 1502 vs, 1437 w, 1386 w, 1333 vw, 1244 s, 1224 s, 1178 vw, 1112 w, 1019 m, 949 m, 918 vs, 825 vs, 817 vs, 775 s, 710 w, 685 vw, 653 vw  $cm^{-1}$ .  $^1H$  NMR (200.13 MHz,  $C_6D_6$ , 295 K):  $\delta$  0.29 (s, 3H,  $SiCH_3$ ), 0.62 (s, 18H,  $Si(CH_3)_2$ ), 2.19 (s, 9H,  $CH_3C_6H_4$ ), 5.28 (s, 10H,  $C_5H_5$ ), 7.01 (d,  $^3J_{HH} = 7.8$  Hz, 6H,  $H^{2,6}$  of  $CH_3C_6H_4$ ), 7.23 (d,  $^3J_{HH} = 7.9$  Hz, 6H,  $H^{3,5}$  of  $CH_3C_6H_4$ ).  $\{^1H\}^{13}C$  NMR (50.3 MHz,  $C_6D_6$ , 295 K):  $\delta$  -14.3 ( $SiCH_3$ ), 3.9 ( $Si(CH_3)_2$ ), 20.8 ( $CH_3C_6H_4$ ), 110.8 ( $C_5H_5$ ), 128.3 ( $C^{2,6}$ ), 129.7 ( $C^{3,5}$ ), 130.3 ( $C^4$ ), 151.0 ( $C^1$ ).  $\{^1H\}^{29}Si$  NMR (39.8 MHz,  $C_6D_6$ , 295 K):  $\delta$  -88.7 ( $SiCH_3$ ), -0.3 ( $Si(CH_3)_2$ ). Anal. Calcd for  $C_{38}H_{52}ClHfN_3Si_4Sn$  [995.83]: C, 45.83; H, 5.26; N, 4.22. Found: C, 45.21; H, 5.04; N, 4.14.

**X-ray Diffraction Study of 4 and 5.** X-ray diffraction data were collected with a Nonius KappaCCD diffractometer using Mo  $K\alpha$  radiation ( $\lambda = 0.71073$  Å). Denzo and Scalepack<sup>22</sup> programs were used for cell refinements and data reduction. The crystal structures of **4** and **5** were solved by direct methods

(20) Hellmann, K. W.; Gade, L. H. *Verfahrenstechnik* **1997**, 31 (5), 70.

(21) Gilman, H.; Rosenberg, S. D. *J. Am. Chem. Soc.* **1952**, 74, 531.

(22) Otwinowski, Z.; Minor, W. In *Methods in Enzymology*, Volume 276, *Macromolecular Crystallography, Part A*; Carter, C. W., Jr., Sweet, R. M., Eds.; Academic Press: New York, 1997; pp 307–326.

Table 2. Crystal Data and Structure Refinement for **4** and **5**

	<b>4</b>	<b>5</b>
empirical formula	C <sub>38</sub> H <sub>52</sub> ClN <sub>3</sub> Si <sub>4</sub> SnZr·C <sub>6</sub> D <sub>6</sub>	C <sub>38</sub> H <sub>52</sub> ClHfN <sub>3</sub> Si <sub>4</sub> Sn·C <sub>6</sub> D <sub>6</sub>
fw	992.69	1079.96
temp (K)	150	150
cryst size (mm)	0.40 × 0.30 × 0.30	0.20 × 0.20 × 0.10
cryst syst	orthorhombic	orthorhombic
space group	<i>P</i> 2 <sub>1</sub> 2 <sub>1</sub> 2 <sub>1</sub>	<i>P</i> 2 <sub>1</sub> 2 <sub>1</sub> 2 <sub>1</sub>
unit cell dimens		
<i>a</i> (Å)	12.32520(10)	12.30500(10)
<i>b</i> (Å)	17.58540(10)	17.56460(10)
<i>c</i> (Å)	21.0750(2)	21.0887(2)
α (deg)	90	90
β (deg)	90	90
γ (deg)	90	90
<i>V</i> (Å <sup>3</sup> )	4567.87(6)	4557.95(6)
<i>Z</i>	4	4
<i>D</i> <sub>calc</sub> (mg cm <sup>−3</sup> )	1.443	1.574
μ(Mo Kα) (mm <sup>−1</sup> )	0.972	3.021
<i>F</i> (000)	2024	2152
2θ <sub>max</sub> (deg)	54.96	50.34
no. of reflns collcd	55527	45411
no. of indepdt reflns	10432	8152
<i>R</i> <sub>int</sub>	0.0282	0.0438
max/min transm	0.2685/0.2249	0.26797/0.23070
no. of data/restraints/params	10432/0/498	8152/0/498
goodness-of-fit on <i>F</i> <sup>2</sup>	1.075	1.076
<i>R</i> <sub>1</sub> [ <i>I</i> > 2σ( <i>F</i> )], <i>wR</i> <sub>2</sub> <sup>a</sup> (all data)	0.0174, 0.0436	0.0227, 0.0472
max. Δρ (e Å <sup>−3</sup> )	0.456/−0.297	0.418/−0.662

$$^a R_1 = \sum ||F_o| - |F_c|| / \sum |F_o| \text{ and } wR_2 = [\sum w(F_o^2 - F_c^2)^2 / \sum w(F_o^2)^2]^{0.5}.$$

using the SIR97<sup>23</sup> and SHELXS97<sup>24</sup> programs with the WinGX<sup>25</sup> graphical user interface. Structure refinements were carried out with SHELXL97.<sup>26</sup> A multiscan absorption correction, based on equivalent reflections (XPRED in SHELXTL v5.1),<sup>27</sup> was applied to all data (*T*<sub>max</sub>/*T*<sub>min</sub> 0.2685/2249, 0.2680/0.2307, for **4** and **5**, respectively). All hydrogen atoms were constrained to ride on their parent atom. Both structures were solved as racemic twins in the orthorhombic space group *P*2<sub>1</sub>2<sub>1</sub>2<sub>1</sub> (Flack parameter 0.459(8) and 0.240(5) for **4** and **5**, respectively).

(23) Altomare, A.; Burla, M. C.; Camalli, M.; Cascarano, G. L.; Giacovazzo, C.; Guagliardi, A.; Moliterni, A. G. G.; Polidori, G.; Spagna, R. *J. Appl. Crystallogr.* **1999**, *32*, 115.

(24) Sheldrick, G. M. *SHELXS97*, Program for Crystal Structure Determination; University of Göttingen: Germany, 1997.

(25) Farrugia, L. J. *J. Appl. Crystallogr.* **1999**, *32*, 837.

(26) Sheldrick, G. M. *SHELXL97*, Program for Crystal Structure Refinement; University of Göttingen: Germany, 1997.

(27) Sheldrick, G. M. *SHELXTL* Version 5.1, Bruker Analytical X-ray Systems; Bruker AXS, Inc.: Madison, WI, 1998.

Details of data collection, refinement, and crystal data are listed in Table 2.

**Acknowledgment.** We thank the European Union (TMR program, network MECATSYN), the Deutsche Forschungsgemeinschaft (SFB 347), the CNRS (France), and the Fonds der Chemischen Industrie for financial support.

**Supporting Information Available:** Text detailing the structure determination and tables of crystallographic data, the positional and thermal parameters, and interatomic distances and angles as well as thermal ellipsoid plots for **4** and **5**. This material is available free of charge via the Internet at <http://pubs.acs.org>.

OM010114Z